ELSEVIER

European Journal of Pharmacology 355 (1998) 103–111

ejp

# Use of a spreadsheet to quantitate the equilibrium binding of an allosteric modulator

Arthur Christopoulos *, Fred Mitchelson

*Department of Pharmaceutical Biology and Pharmacology, Victorian College of Pharmacy (Monash University), 381 Royal Pde., Parkville 3052, Victoria, Australia*

Received 23 March 1998; revised 22 June 1998; accepted 23 June 1998

**Abstract**

Using the program Microsoft EXCEL, a spreadsheet was developed for constrained, simultaneous analysis of multiple datasets obtained from equilibrium binding experiments, according to an allosteric model of interaction. This approach was used to quantitate the interaction between the modulator (heptane-1,7-bis (dimethyl 3′-phthalimidopropyl) ammonium bromide) ($C_7$/3-phth) and the radioligands [$^3$H]*N*-methylscopolamine and [$^3$H]quinuclidinyl benzilate at cortical and atrial muscarinic receptors. The interaction between various concentrations of the radioligands and $C_7$/3-phth, in the guinea pig atrium and in the rat cerebral cortex, could be well described by the allosteric model. The affinity of $C_7$/3-phth for unoccupied atrial receptors was significantly higher than for cortical receptors. The negative cooperativity between [$^3$H]quinuclidinyl benzilate and the modulator was higher in cortex than that between the modulator and [$^3$H]*N*-methylscopolamine. It is suggested that the described method has wide applicability because of the extensive availability of spreadsheet programs, the analytical advantages offered by constrained, simultaneous nonlinear regression and the ability to adapt the spreadsheet to almost any model of ligand–receptor interaction. 

*Keywords:* Allosteric interaction; Muscarinic receptor; Spreadsheet; Regression nonlinear; $C_7$/3-phth

## 1. Introduction

Muscarinic acetylcholine receptors belong to the superfamily of G protein-coupled receptors, and the existence of allosteric binding sites on these proteins has been acknowledged for some time (see Lee and El-Fakahany, 1991; Tucek and Proška, 1995; Christopoulos et al., 1998). Positive cooperativity manifested in equilibrium binding experiments is readily detected, as the allosteric modulator causes enhancement of radioligand binding (Tucek et al., 1990). However, negatively cooperative interactions may appear indistinguishable from competitive antagonism if the degree of negative cooperativity is high (Ehlert, 1988). In certain instances, repeating the experiment in the presence of an increased radioligand concentration may allow the deviations from competitive behaviour to be more readily visualized (Stockton et al., 1983; Lee and El-Fakahany, 1991). Additionally, if a minimum of two separate experiments are performed on the same tissue preparation (e.g., homogenate, intact cells, etc.), each utilizing a different fixed concentration of radioligand, then analytical advantages may also be obtained. This is so because a constrained, simultaneous analysis of the entire family of datasets can give more accurate estimates of the degree of cooperativity characterizing the interaction and the affinity of the modulator for the unliganded receptor than experiments utilizing different tissue preparations for each assay. Unfortunately, this particular curve-fitting feature is often missing from a number of dedicated, commercially available data analysis packages.

Recently, Bowen and Jerman (1995) described how a readily available spreadsheet program, Microsoft Excel, could be utilized to perform iterative, least-squares, nonlinear regression analysis. A particularly appealing feature of this package is the ability to simultaneously fit families of related datasets, with or without constraining the parame-

* Corresponding author. Present address: Neuroscience Research in Psychiatry, Box 392, Mayo Memorial, University of Minnesota Medical School, Minneapolis, MN 55455, USA. Tel.: +1-612-624-2687; Fax: +1-612-624-8935; E-mail: christo@lenti.med.umn.edu

0014-2999/98/$19.00 

ters to be shared across the datasets, because it offers the advantage of extracting more information from the experimental data. Constraining certain parameters to be shared by all datasets will increase the degrees of freedom and the accuracy of the final parameter estimates, provided that the underlying model is correct (De Lean et al., 1978; Kenakin, 1997). Additionally, models with more than one independent variable can be accommodated.

Previous experiments with the muscarinic receptor antagonist, (heptane-1,7-bis (dimethyl 3′-phthalimidopropyl) ammonium bromide) ($C_7$/3-phth), against the binding of the antagonist, [$^3$H]quinuclidinyl benzilate in rat cortex, yielded inhibition curves that could be adequately fitted to a two-site, competitive binding model (Christopoulos et al., 1993). However, functional and dissociation kinetic studies have identified the former agent as possessing allosteric binding properties (Mitchelson, 1975; Christopoulos and Mitchelson, 1994; Lanzafame et al., 1996). Therefore, the aim of the present study was to adapt a simple scheme of allosteric interaction at G protein-coupled receptors for constrained, simultaneous, nonlinear regression analysis with the spreadsheet program, Microsoft EXCEL, and to use this template to quantitate the cooperativity manifest in the interaction between $C_7$/3-phth and the radioligands [$^3$H]*N*-methylscopolamine and [$^3$H]quinuclidinyl benzilate.

## 2. Materials and methods

### 2.1. Preparation of tissue homogenates

Hooded Wistar rats of either sex (200–300 g) were killed by decapitation and their brains rapidly removed and placed in ice-cold phosphate buffer (50 mM $Na_2HPO_4$; pH 7.4). The cortex was dissected out from the rest of the brain, blotted, weighed and homogenized in 15 volumes of the phosphate buffer using a Potter Elvehjem homogenizer (20 strokes). Homogenates were then centrifuged at −4°C for 10 min at $1000 \times g$ using a Sorvall RC-2B refrigerated centrifuge and the supernatant was re-centrifuged for $2 \times$ 20 min periods at $40\,000 \times g$. The pellet from this extra centrifugation was re-suspended in ice-cold phosphate buffer (50 ml/g original wet weight) and used for the binding assays.

Guinea pigs, of either sex, were killed by a blow to the head followed by exsanguination. Hearts were then placed in ice-cold phosphate buffer. Atria were separated from ventricles, blotted dry, minced finely, weighed, mixed with 15 volumes of buffer and homogenized in an Ultra-Turrax set at $0.75 \times$ maximum speed for $2 \times 30$ s, with a 30 s period of cooling on ice between homogenizations. Following centrifugation at −4°C for 10 min at $1000 \times g$, the supernatant was collected and subsequently used in the binding studies.

### 2.2. Radioligand binding assays

Inhibition binding studies were conducted employing a 'multiple-curve' (Leff et al., 1990) design. Briefly, each experiment, performed on a single tissue homogenate, utilized a three-curve assay. For construction of each individual curve, increasing concentrations of $C_7$/3-phth were incubated with homogenate and a fixed concentration of radioligand. The fixed radioligand concentration was different (as indicated in Section 3) for each inhibition curve. Incubation (1 ml total volume/tube) was then allowed to proceed for 1 h at 37°C before termination, by vacuum filtration. Non-specific binding was defined using atropine (10 μM). Radioactivity was determined by scintillation counting, as described previously (Christopoulos and Mitchelson, 1994).

### 2.3. Data analysis

Unless otherwise stated, a custom-written EXCEL template (see Appendix A) was used to simultaneously analyze the entire family of inhibition curves, obtained from each experiment utilizing increasing concentrations of modulator against various fixed concentrations of radioligand, according to the following equation (Ehlert, 1988):

$$\frac{Y}{Y_0} = \frac{[A]}{[A] + K_A \cdot \left( \frac{K_Z + [Z]}{K_Z + [Z]/\alpha} \right)} \quad (1)$$

where $Y/Y_0$ represents fractional receptor occupancy, $[A]$ and $[Z]$ represent the concentrations, $K_A$ and $K_Z$ represent the equilibrium dissociation constants of the radioligand and allosteric modulator, respectively, and $\alpha$ represents the heterotropic cooperativity factor between the two ligands. This latter value is a quantitative estimate of the magnitude by which the binding of one ligand to its site on the receptor alters the affinity of the other ligand, and vice versa. Values of $\alpha < 1$ denote positive cooperativity, whereas values of $\alpha > 1$ denote negative cooperativity (Ehlert, 1988). The values of $[A]$, $[Z]$ and $K_A$ were entered, and $K_Z$ was estimated, as logarithms. Monte Carlo simulations (not shown) indicate that $\alpha$ values follow an approximate Gaussian distribution only when converted to logarithms, therefore the latter parameter was also converted to its logarithmic equivalent before application of statistical testing. In each instance, the parameters $\alpha$ and $K_Z$ were constrained to be shared by all curves (see Appendix A).

Data shown are the mean ± S.E.M. For clarity, the geometric mean associated with the estimates of log $\alpha$ is also given in parentheses. Comparisons between means were by Student's *t*-test or One-way analysis of variance (ANOVA), as appropriate. Unless otherwise stated, values of $P < 0.05$ were taken as significant. Goodness-of-fit was assessed by using Excel to plot the residuals, allowing for a runs test to be performed, and an $R^2$ (coefficient of

determination) value was also calculated (see Motulsky, 1995), as the spreadsheet is able to generate the variance of the datasets.

### 2.4. Drugs

[$^3$H](−)-*N*-methyl scopolamine methyl chloride and [$^3$H](−)-quinuclidinyl benzilate (Amersham, UK); $C_7$/3-phth (heptane-1,7-bis (dimethyl 3′-phthalimidopropyl) ammonium bromide) (IDT, Melbourne, Australia); atropine sulphate (Sigma, St. Louis, MO, USA).

## 3. Results

### 3.1. $C_7$/3-phth *vs.* [$^3$H]*N* − methylscopolamine

Experiments conducted with $C_7$/3-phth against the binding of the orthosteric antagonist [$^3$H]*N*-methylscopolamine are shown in Fig. 1. In the case of the studies conducted in guinea pig atria, three separate experiments, each utilizing [$^3$H]*N*-methylscopolamine concentrations of 0.1, 0.3 and 3 nM (Log $K_A = -9.52$), were performed and analyzed using the Excel template for negative cooperativity. The Log $K_Z$ for $C_7$/3-phth in this tissue (Fig. 1A) was $-7.24 \pm 0.35$ and the Log $\alpha$ value was $0.79 \pm 0.03$ (geometric mean, GM: 6.2). Similar experiments conducted using rat cortical homogenates (Fig. 1B) yielded a Log $K_Z$ of $-6.18 \pm 0.24$ and a Log $\alpha$ value of $0.69 \pm 0.02$ (GM: 4.9; $n = 3$).

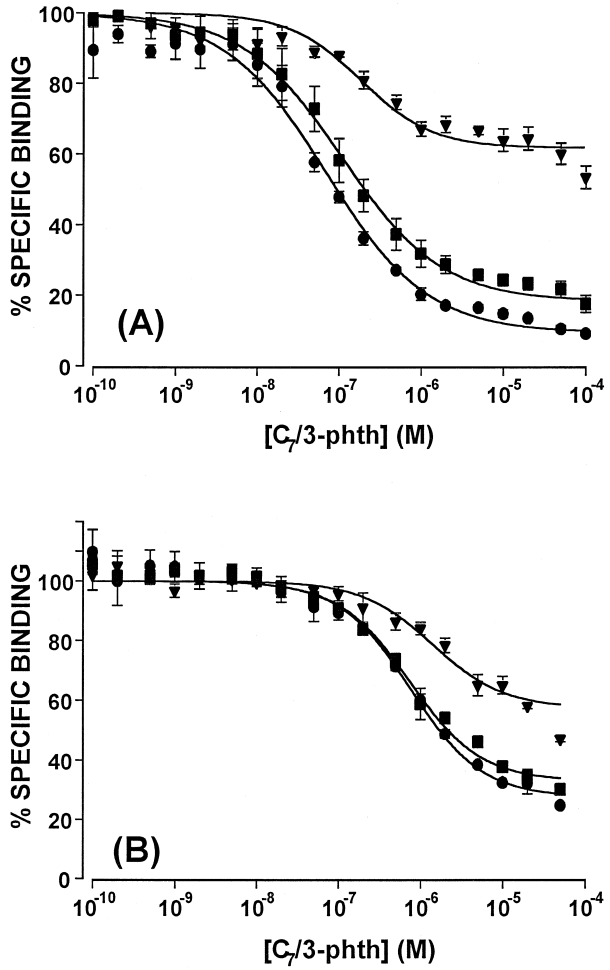


Fig. 1. Effect of $C_7$/3-phth on the equilibrium binding of [$^3$H]*N*-methylscopolamine, 0.1 nM (●), 0.3 nM (■) and 3 nM (▼) in (A) guinea pig atria and (B) rat cortex. Homogenates were incubated in 50 mM phosphate buffer, pH 7.4, at 37°C for 1 h. Normalized curves represent constrained simultaneous fits, using a Microsoft Excel template, for the interaction between $C_7$/3-phth and [$^3$H]*N*-methylscopolamine.

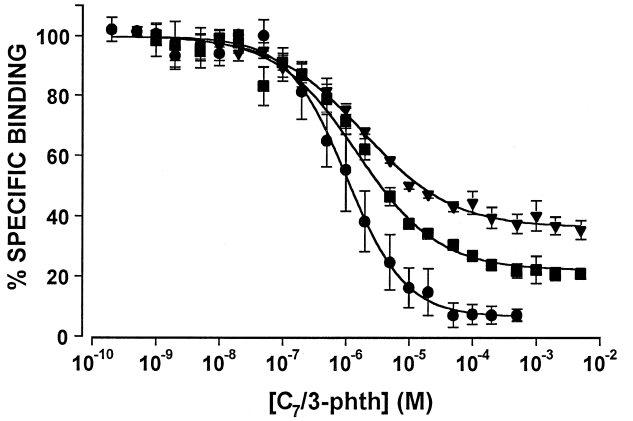


Fig. 2. Effect of $C_7$/3-phth on the equilibrium binding of [$^3$H]quinuclidinyl benzilate 50 pM (●), 200 pM (■) and 500 pM (▼) in rat cortex. Homogenates were incubated in 50 mM phosphate buffer, pH 7.4, at 37°C for 1 h. Normalized curves represent constrained simultaneous fits, using a Microsoft Excel template, for the interaction between $C_7$/3-phth and [$^3$H]quinuclidinyl benzilate.

### 3.2. $C_7$/3-phth *vs.* [$^3$H] quinuclidinyl benzilate

Experiments were also conducted with $C_7$/3-phth against [$^3$H]quinuclidinyl benzilate in rat cortex. The results are shown in Fig. 2, where it may be seen that $C_7$/3-phth displayed a progressive inability to maximally inhibit the binding of increasing concentrations (50, 200, 500 pM) of [$^3$H]quinuclidinyl benzilate (Log $K_A = -10.30$). Log $K_Z$ was estimated as $-6.33 \pm 0.77$ and Log $\alpha$ as $1.19 \pm 0.03$ (GM: 15.5; $n = 3$).

In both the [$^3$H]*N*-methylscopolamine and [$^3$H]quinuclidinyl benzilate binding studies, the runs test gave values of $P > 0.05$, signifying that the data did not deviate significantly from the chosen model. Values for $R^2$ ranged from 0.95 to 0.99, indicating an excellent goodness-of-fit. Thus, the interaction between $C_7$/3-phth and either [$^3$H]*N*-methylscopolamine or [$^3$H]quinuclidinyl benzilate was compatible with a simple allosteric model of interaction.

A one-way ANOVA found that the estimates of Log $K_Z$ for $C_7$/3-phth differed significantly between atria and cortex ($P < 0.05$), but the two estimates obtained in the cortex did not. The degree of negative cooperativity with [$^3$H]quinuclidinyl benzilate was significantly greater ($P < 0.05$) than that with [$^3$H]*N*-methylscopolamine in the cor-

tex, although the value for the interaction between $C_7$/3-phth and [$^3$H]*N*-methylscopolamine in the two tissues was not ($P > 0.05$).

## 4. Discussion

The allosteric ternary complex model is an example of a non-competitive drug-receptor occupancy model. The quantitation of allosteric phenomena in steady-state or equilibrium binding assays depends on the ability to reliably and consistently evaluate complex binding curves with a minimum of data transformation. Nonlinear regression analysis allows for such an evaluation, and the method presented in Appendix A to this paper demonstrates a practical application of this approach using the popular spreadsheet program, Microsoft Excel. The main advantages offered by this program, compared to more dedicated data analysis packages, is its ability to process large amounts of raw data, to fit these raw data to almost any model and to accommodate multiple independent variables (as found in the analysis of allosteric equilibrium binding data). Of particular utility to the current study is the ability to program Excel to simultaneously analyze families of related datasets, allowing for parameters to be shared between the datasets.

The use of simultaneous analysis of families of concentration–response curves was pioneered by Waud (Parker and Waud, 1971; Waud and Parker, 1971; Waud, 1975; Waud et al., 1978). The advantages of this method of data analysis have been extensively explored by others (De Lean et al., 1978; Munson and Rodbard, 1980; Munson, 1983) and applied to the study of a variety of drug–receptor models. For example, constrained simultaneous analyses have been conducted based on the occupation model of agonism in both isolated tissue experiments (Waud, 1975) and radioligand binding studies (Munson and Rodbard, 1980), as well as analyses based on the operational model of agonism (Black and Leff, 1983; Leff et al., 1990) and the allosteric ternary complex model (Lazareno and Birdsall, 1995). In each instance, however, dedicated and specialized, programmable computer packages were utilized, and these may not be readily available to many researchers. Microsoft Excel, however, is one of the world's most popular spreadsheet packages, and Bowen et al. (1994) have demonstrated how this program may be used to simultaneously analyze agonist concentration-effect data according to the operational model of Black and Leff (1983).

Although the initial configuration of the spreadsheet template, as outlined in Appendix A, may appear laborious, it is worth noting that Excel contains an extensive macro language that allows for a high degree of automation in data handling and processing. Also, the 'programming' involved in spreadsheet configuration is quite straightforward, while at the same time allowing the user to develop a 'feel' for nonlinear modeling/analysis. The merits of this type of 'hands-on' approach to data analysis have been highlighted by Waud (1987).

Unfortunately, the spreadsheet approach presented does not allow for the generation of estimates of the standard errors associated with each parameter after an individual fit. However, even programs that do generate standard errors for nonlinear models must employ linearizing assumptions in the process, and these generated errors often underestimate the true error (Motulsky and Ransnas, 1987). Nevertheless, the lack of this feature in the spreadsheet package implies that the choice of experimental design can dictate the applicability of the spreadsheet approach to data analysis. Data from single-curve experimental designs may be analyzed, parameter estimates may be derived, the experiment may be repeated a number of times and means with associated standard errors may be calculated. However, this scheme cannot take inter-tissue variability into account if different tissues are used to generate 'control' curves from those used to generate 'treated' curves. On the other hand, a multiple-curve design allowing, at least, one 'control' and one 'treated' curve per tissue, together with associated simultaneous data analysis, places more realistic constraints on the values parameters may take; hence, greater reliability in the interpretation of the biological meaning of the final estimates. Replication of this type of experiment allows for a more confident and realistic determination of standard error. For the purposes of the present study, 'control' and 'treated' curves may be taken as representing 'low' and 'high' radioligand concentrations, respectively.

The application of a multiple-curve experimental design to the study of the interaction between $C_7$/3-phth and either [$^3$H]*N*-methylscopolamine or [$^3$H]quinuclidinyl benzilate resulted in the determination of estimates of affinity and cooperativity for this modulator in atrial and cortical tissues. The data did not significantly deviate from, and were well-described by, an allosteric model, as evidenced by the $R^2$ values. The errors associated with each of the generated parameter estimates were also reasonable. It appears, therefore, that $C_7$/3-phth exhibits a higher degree of negative cooperativity with [$^3$H]quinuclidinyl benzilate than with [$^3$H]*N*-methylscopolamine. This may explain why previous studies conducted with low, fixed concentrations of the former radioligand, as is common for traditional competition binding assays, may fail to differentiate allosteric inhibition from competition at non-interacting, homo- or heterogeneous receptor populations (Christopoulos et al., 1993).

With regard to the [$^3$H]*N*-methylscopolamine experiments, $C_7$/3-phth displayed higher affinity for guinea pig atrial muscarinic receptors than for rat cerebral cortical receptors, in agreement with previous results (Christopoulos et al., 1993; Christopoulos and Mitchelson, 1994). However, the degree of negative cooperativity appeared to

be slightly higher in atria than in cortex, although the difference was not significant ($P > 0.05$). Atrial muscarinic receptors are believed to be comprised almost exclusively of the $M_2$ subtype (Caulfield, 1993), allowing for a relatively straightforward interpretation of the results from the present experiments, conducted in this tissue. In contrast, the cerebral cortex is believed to contain a heterogeneous mix of the muscarinic $M_1$–$M_4$ receptor subtypes, represented mainly by the muscarinic $M_1$ and $M_4$ types (Waelbroeck et al., 1990; Caulfield, 1993). Additionally, depending on the radioligand employed, the proportions of the various subtypes detected may vary (Christopoulos et al., 1993). The fact that the inhibition binding isotherms, utilizing [$^3$H]*N*-methylscopolamine or [$^3$H]quinuclidinyl benzilate, could be well-described by a simple one-receptor allosteric ternary complex model and, furthermore, that the estimates of modulator affinity did not differ significantly between these assays suggests that the predominant subtype contributing to the observed binding profile may have been the muscarinic $M_1$ receptor. This finding is also supported by preliminary studies using cloned human muscarinic $M_1$ receptors in a recombinant expression system, that have also shown an almost identical binding profile for $C_7$/3-phth against [$^3$H]*N*-methylscopolamine under similar assay conditions (A. Christopoulos, F. Mitchelson and E.E. El-Fakahany, unpublished observations).

In conclusion, the present study has outlined a method for performing constrained, simultaneous, nonlinear regression analysis using a spreadsheet program to quantitate allosteric interactions. This approach has been applied to the quantitation of the allosteric binding properties of $C_7$/3-phth at atrial and cortical muscarinic receptors, resulting in the finding of a significantly higher affinity of the modulator for the unoccupied atrial receptors, compared to the cortical receptors. The negative cooperativity factors were found to vary with the radioligand employed, and were higher with [$^3$H]quinuclidinyl benzilate than with [$^3$H]*N*-methylscopolamine.

**Acknowledgements**

The authors are grateful to Prof. Esam E. El-Fakahany for critical review of the manuscript. This work was supported by a grant from the National Health and Medical Research Council of Australia.

## Appendix A. The model

The simplest model that is able to describe allosteric interactions at G protein-coupled receptors is the ternary complex model, that allows for the interaction between two ligands, via topographically distinct binding sites, on the same receptor protein (Stockton et al., 1983; Ehlert, 1988):

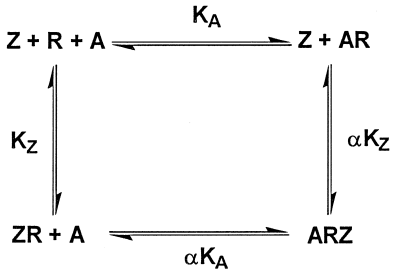


where $[A]$ and $[Z]$ represent the concentrations, $K_A$ and $K_Z$ represent the equilibrium dissociation constants of the radioligand and allosteric modulator, respectively, and $\alpha$ represents the heterotropic cooperativity factor between the two ligands. From the model, the fractional binding ($Y/Y_0$) of A, in the presence of Z is shown in Eq. (1) of Section 2.3. This equation describes a saturation binding isotherm for the orthosteric ligand, A, in the presence of a fixed concentration of modulator, Z. Binding experiments are more commonly performed by measuring the effects of increasing concentrations of modulator on the binding of a fixed concentration of radiolabelled orthosteric ligand.

When attempting to fit radioligand binding isotherms conducted under these latter conditions, the following relationships are useful:bound A in the absence of Z,

$$\frac{Y}{Y_0} = \frac{[A]}{[A] + K_A} \quad \text{(A1)}$$

bound A in the presence of an 'infinite' concentration of Z,

$$\frac{Y}{Y_0} = \frac{[A]}{[A] + \alpha K_A} \quad \text{(A2)}$$

midpoint location parameter,

$$[Z] = \frac{\alpha K_Z([A] + K_A)}{[A] + \alpha K_A} \quad \text{(A3)}$$

Experimental binding data are most often expressed in terms of percentage specific binding, or as counts (or disintegrations) per minute. Listed in Table 1 are the two groups of equations (one group for negative, the other for positive cooperativity, based on Eqs. (A1), (A2) and (A3)) that may be used to directly define an allosteric curve fit to such data.

All curves are generated from a point representing the binding of the initial, fixed concentration of radioligand in the absence of modulator ('max' for a negatively cooperative system, 'min' for a positively cooperative system). Equations (a) and (b) in Table 1 define the level of binding to which the curves subsequently asymptote, at 'infinite' concentrations of modulator. Equations (c) and (d), defining the midpoint location parameter of the curves, may be

Table 1
Suite of equations that may be utilized to directly fit a simple allosteric ternary complex model to experimental binding data derived from equilibrium binding studies

| Equations for negative cooperativity | Equations for positive cooperativity |
|---|---|
| (a) $\min = (\max(A + K_A))/(A + \alpha K_A)$ | (b) $\max = (\min(A + K_A))/(A + \alpha K_A)$ |
| (c) $Z_{mid} = (\alpha K_Z(A + K_A))/(A + \alpha K_A)$ | (d) $Z_{mid} = (\alpha K_Z(A + K_A))/(A + \alpha K_A)$ |
| (e) $Y = \min + (\max - \min)/(1 + 10^{(\mathrm{Log}Z - LogZ_{mid})})$ | (f) $Y = \min + (\max - \min)/(1 + 10^{(LogZ_{mid} - LogZ)})$ |
| $(\alpha > 1)$ | $(\alpha < 1)$ |

shown to be identical. The final two equations, (e) and (f), allow the model to be fitted as a four-parameter logistic function. This function has found widespread application in pharmacological analysis because it is mathematically simple, manageable, robust and allows for sigmoid concentration-effect/concentration-binding curves which are often found in biological systems (Waud and Parker, 1971; Waud, 1975; De Lean et al., 1978; Black and Leff, 1983).

### A.1. Entering data

Microsoft Excel can handle any equation of the form $y = f(x)$, containing up to 200 parameters (Bowen and Jerman, 1995). Thus, data must be tabulated in terms of $y$, the dependent variable, and $x$, the independent variable. The equations to be used in the present analysis are those listed in Table 1. However, before entering the relevant equations into the appropriate cells of the spreadsheet, it is prudent to re-cast some of the parameters as logarithms. This is necessary because many biological parameters, including dissociation constants, have been shown to follow a log–normal, rather than a normal, distribution (Fleming et al., 1972; De Lean et al., 1982; Hancock et al., 1988; Hulme and Birdsall, 1992). Thus, $[Z]$, $K_A$ and $K_Z$ would need to be re-cast as $10^{\log[Z]}$, $10^{\mathrm{Log}K_A}$ and $10^{\mathrm{Log}K_Z}$, respectively. The cooperativity factor, $\alpha$, may also be reparameterized as $10^{\mathrm{Log}\alpha}$, but in the present study, this transformation of $\alpha$ values has been performed after the estimation of the parameter via the curve-fitting procedure. In any instance, standard statistical analyses, which assume a normal distribution for parameters, should only be employed when the appropriate parameter transformations have been undertaken.

Fig. 3 is a spreadsheet template that has been constructed to simultaneously analyze a family of two separate, simulated datasets. The datasets are based on a negatively cooperative model with a Log $K_Z$ of $-7$ and an $\alpha$ of 10. Random 'noise' was also added to the datasets, thus simulating experimental error.

| | A | B | C | D | E | F | G | H | I | J |
|---|---|---|---|---|---|---|---|---|---|---|
| 1 | | | Dataset 1 | | | | | Dataset 2 | | |
| 2 | | Log[Z] | Y (Obs.) | Y (Pred.) | Sqr. Diff. | | Log[Z] | Y (Obs.) | Y (Pred.) | Sqr. Diff. |
| 3 | | -10.00 | 100.76 | 99.54 | 1.49 | | -10.00 | 103.12 | 99.92 | 10.27 |
| 4 | | -9.00 | 94.75 | 95.57 | 0.67 | | -9.00 | 103.55 | 99.16 | 19.24 |
| 5 | | -8.00 | 97.37 | 69.57 | 773.22 | | -8.00 | 98.78 | 92.63 | 37.80 |
| 6 | | -7.00 | 69.20 | 26.32 | 1838.68 | | -7.00 | 90.06 | 66.27 | 566.20 |
| 7 | | -6.00 | 31.76 | 14.11 | 311.48 | | -6.00 | 70 | 47.47 | 507.73 |
| 8 | | -5.00 | 18.97 | 12.66 | 39.76 | | -5.00 | 61.56 | 44.37 | 295.59 |
| 9 | | -4.00 | 17.47 | 12.52 | 24.56 | | -4.00 | 53.9 | 44.04 | 97.28 |
| 10 | | | | | | | | | | |
| 11 | | | | Logmid1 | -7.73 | | | | Logmid2 | -7.18 |
| 12 | | | | SS1 | 2989.86 | | | | SS2 | 1534.11 |
| 13 | | | | min1 | 12.50 | | | | min2 | 44.00 |
| 14 | | | | LogA1 | -9.00 | | | | LogA2 | -8.00 |
| 15 | | | | | | | | | | |
| 16 | | | Shared Parameters: | | | | | | | |
| 17 | | | | max | 100 | | | | | |
| 18 | | | | LogKA | -9 | | | | | |
| 19 | | | | LogKZ | -8 | | | | | |
| 20 | | | | α | 15 | | | | | |
| 21 | | | | | | | | | | |
| 22 | | | Total SSqr: | | | | | | | |
| 23 | | | | 4523.97 | | | | | | |

Fig. 3. Spreadsheet template for the simultaneous analysis of a family of two equilibrium binding datasets according to an allosteric ternary complex model. Data and parameter estimates shown are those before minimization. Note the values for Log $K_Z$, $\alpha$ and Total SSqr.

For each dataset, four columns need to be set aside on the spreadsheet. This example will concentrate on dataset 1 of Fig. 3, as the steps are similar for the other dataset. The first column is headed 'Log[$Z$]' and contains the values of the various concentrations of allosteric modulator, Z, entered as logarithms. This column, thus, contains the independent variable. The second column, '$Y$ (Obs.)' contains the dependent variable, i.e., the experimental observations, expressed in terms of percentage specific binding. The third column, '$Y$ (Pred.)', contains the formula for the general logistic function which calculates the predicted binding, based on the model and the initial parameter estimates (see below). The fourth column, 'Sqr. Diff.', contains the formula for calculating the square of the differences between each pair of observed/predicted values.

In addition, each dataset requires a number of other cells to be defined that contain the parameters utilized in the regression procedure. In Fig. 3, for example, cell E11 contains the formula for 'Logmid1', based on equation (c), cell E12 contains the formula for calculating 'SS1', the sum of the square of the differences listed above in column E, while cell E13 contains the formula defining 'min1', based on equation (a). Cell E14 contains 'logA1', the value of the logarithm of the fixed concentration of radioligand that was employed in the experiment.

The final set of cells that need to be set aside are those that contain parameter values to be shared by both datasets. Cell E17 contains the value for 'max', the starting point of the curves (in the absence of modulator), set as 100% specific binding. Note that if counts- or disintegrations/min are employed, instead of specific binding, then 'max' cannot be a shared parameter, but must be specified for each dataset (e.g., 'max1', 'max2'). Cell E18 contains 'LogKA', the logarithm of the radioligand dissociation constant, which is determined separately and fixed in this analysis. Cells E19 and E20 contain 'LogKZ', the logarithm of the dissociation constant of the modulator, and '$\alpha$', the cooperativity factor, respectively. These are initially entered as approximate estimates and are improved by the iterative minimization algorithm. Finally, cell D23, 'Total SSqr', contains the formula for calculating the total sum-of-squares from both datasets. This is the target cell whose value the minimization algorithm attempts to reduce.

### *A.2. Entering formulae and parameter estimates*

All formulae entered into cells of the EXCEL program begin with an '=' sign and need to be written in a linear form as follows:

- logistic function (begin in cell D3): = min1 + ((max − min1)/(1 + (10 ^Log $Z$1 − Logmid1)))) this formula is copied through to cell D9
- square-difference (begin in cell E3): = $(C3 - D3)^2$

  this is repeated for each corresponding C/D cell pair, down column E. If different forms of data weighting

| | | A | B | C | D | E | F | G | H | I | J |
|---|---|---|---|---|---|---|---|---|---|---|---|
| 1 | 1 | | | Dataset 1 | | | | | Dataset 2 | | |
| 2 | 2 | | Log[Z] | Y (Obs.) | Y (Pred.) | Sqr. Diff. | | Log[Z] | Y (Obs.) | Y (Pred.) | Sqr. Diff. |
| 3 | 3 | | -10.00 | 100.76 | 99.95 | 0.65 | | -10.00 | 103.12 | 99.99 | 9.79 |
| 4 | 4 | | -9.00 | 94.75 | 99.51 | 22.67 | | -9.00 | 103.55 | 99.91 | 13.24 |
| 5 | 6 | | -8.00 | 97.37 | 95.39 | 3.93 | | -8.00 | 98.78 | 99.13 | 0.12 |
| 6 | 8 | | -7.00 | 69.20 | 69.48 | 0.08 | | -7.00 | 90.06 | 92.60 | 6.47 |
| 7 | 10 | | -6.00 | 31.76 | 30.30 | 2.13 | | -6.00 | 70 | 70.51 | 0.26 |
| 8 | 12 | | -5.00 | 18.97 | 20.03 | 1.13 | | -5.00 | 61.56 | 57.94 | 13.07 |
| 9 | 14 | | -4.00 | 17.47 | 18.84 | 1.86 | | -4.00 | 53.9 | 56.07 | 4.72 |
| 10 | 15 | | | | | | | | | | |
| 11 | 16 | | | | Logmid1 | -6.78 | | | | Logmid2 | -6.30 |
| 12 | 17 | | | | SS1 | 32.45 | | | | SS2 | 47.68 |
| 13 | 18 | | | | min1 | 18.70 | | | | min2 | 55.85 |
| 14 | 19 | | | | LogA1 | -9.00 | | | | LogA2 | -8.00 |
| 15 | 20 | | | | | | | | | | |
| 16 | 21 | | | Shared Parameters: | | | | | | | |
| 17 | 22 | | | | max | 100 | | | | | |
| 18 | 23 | | | | LogKA | -9 | | | | | |
| 19 | 24 | | | | LogKZ | -7.04 | | | | | |
| 20 | 25 | | | | α | 9.69 | | | | | |
| 21 | 26 | | | | | | | | | | |
| 22 | 27 | | | Total SSqr: | | | | | | | |
| 23 | 28 | | | | 80.13 | | | | | | |

Fig. 4. Spreadsheet template for the simultaneous analysis of a family of two equilibrium binding datasets according to an allosteric ternary complex model. Data and parameter estimates shown are those after minimization. Note the final values for Log $K_Z$, $\alpha$ and Total SSqr.

are required, then the formula in this column may be modified accordingly (see Bowen and Jerman, 1995).

- midpoint location parameter (cell E11):
  $= \text{Log10}((a * (10\ \text{^Log}\ KZ) * ((10\ \text{^Log}\ A1) + (10\ \text{^Log}\ KA))) / ((10\ \text{^Log}\ A1 + (a * (10\ \text{^Log}\ KA))))$

- sum-of-squares for dataset (cell E12): $= \sum(E3{:}E9)$

- curve minimum asymptote (cell E13):
  $= (\max * ((10\ \text{^Log}\ A1) + (10\ \text{^Log}\ KA))) / ((10\ \text{^Log}\ A1) + (a * (10\ \text{^Log}\ KA)))$

- total sum-of-squares, both datasets (cell D23):
  $= SS1 + SS2$

Fixed values (LogA1, LogKA, max) and initial estimates (LogKZ, $\alpha$) are entered in the appropriate cells.

### *A.3. Defining names*

For Excel to recognize names assigned to data columns, cells containing formulae, parameter values and parameter estimates, the 'Insert → Names' command, found as a pull-down menu bar item, must be used to define them.

Thus, the entire data array from B3:B9 is highlighted and defined as 'LogZ1'. This is preferable to 'LogZ' because each dataset may contain a different range of modulator concentrations.

The remaining cells of interest are similarly defined by selecting the cell containing the desired value or formula, choosing the 'Insert → Names' command, and entering the appropriate definition. In Fig. 3, the definitions entered were the same as those on the labels adjacent to each cell, except for the total sum-of-squares cell (D23), which was defined as 'TotalSSqr'. Note, the '*Y* (Obs.)', '*Y* (Pred.)' and 'Sqr. Diff.' columns require no definition.

### *A.4. Minimization using the solver function*

The Solver function of Excel is a powerful tool that is able to find the optimum value for a particular cell (the 'Target Cell') by adjusting the values of several, selected cells (containing the 'Decision Variables') in an iterative manner. The Solver actually uses two minimization algorithms. One is a simplex algorithm, used for linear problems, while the other is a generalized reduced-gradient algorithm, used for nonlinear problems.

The Solver command is an EXCEL add-in that may be found in the 'Tools' pull-down menu. Opening the Solver function will bring up a dialog box that requests the Solver parameters. The cell to be minimized (i.e., TotalSSqr; D23) is entered in the 'Set Cell' box and the 'Min' option is selected at the 'Equal to: ' prompt; specifying that the desired optimization procedure is a minimization. The names of the cells containing the decision variables (LogKZ, $\alpha$) are entered in the 'By Changing Cells:' box. Solver even allows for some constraints to be placed on the upper and/or lower bounds of values that a parameter is allowed to take. Selecting the 'Solve' button then starts the optimization process. Once the fit has converged to a minimum, the program allows the user to save the values and, if desired, generate reports on various aspects of the minimization procedure.

Fig. 4 shows the same spreadsheet template as in Fig. 3, but after the minimization process. Note the final estimates of Log $K_Z$, $-7.04$, and $\alpha$, 9.69. The values in the '*Y* (Pred.)' columns now define the final, generated curves for each experimental dataset, based on the best common fit to the model. Excel can readily use these values to generate graphs of the data.

## References


Black, J.W., Leff, P., 1983. Operational models of pharmacological agonism. Proc. R. Soc. London B 220, 141–162.

Bowen, W.P., Jerman, J.C., 1995. Nonlinear regression using spreadsheets. Trends Pharmacol. Sci. 16, 413–417.

Bowen, W.P., Jerman, J.C., Baxter, G.S., 1994. OPTIMA: simultaneous fitting of response curves to the operational model of agonism with Microsoft EXCEL. Br. J. Pharmacol. 112, 659 pp.

Caulfield, M.P., 1993. Muscarinic receptors—characterization, coupling and function. Pharmacol. Ther. 58, 319–379.

Christopoulos, A., Mitchelson, F., 1994. Assessment of the allosteric interactions of the bisquaternary heptane-1,7-bis-(dimethyl-3′-phthalimidopropyl)-ammonium bromide at $M_1$ and $M_2$ muscarine receptors. Mol. Pharmacol. 46, 105–114.

Christopoulos, A., Loiacono, R., Mitchelson, F., 1993. Binding of the muscarine receptor antagonist heptane-1,7-bis-(dimethyl-3′-phthalimidopropyl)-ammonium bromide at cholinoceptor sites. Eur. J. Pharmacol. (Mol. Pharmacol. Sect.) 246, 1–8.

Christopoulos, A., Lanzafame, A., Mitchelson, F., 1998. Allosteric interactions at muscarinic cholinoceptors. Clin. Exp. Pharmacol. Physiol. 25, 184–194.

De Lean, A., Munson, P.J., Rodbard, D., 1978. Simultaneous analysis of families of sigmoidal curves: application to bioassay, radioligand assay, and physiological dose–response curves. Am. J. Physiol. 253, E97–E102.

De Lean, A., Hancock, A.A., Lefkowitz, R.J., 1982. Validation and statistical analysis of a computer modelling method of quantitative analysis of radioligand binding data for a mixture of pharmacological receptor subtypes. Mol. Pharmacol. 21, 5–16.

Ehlert, F.J., 1988. Estimation of the affinities of allosteric ligands using radioligand binding and pharmacological null methods. Mol. Pharmacol. 33, 187–194.

Fleming, W.W., Westfall, D.P., De La Lande, I.S., Jellet, L.B., 1972. Log–normal distribution of equieffective doses of norepinephrine and acetylcholine in several tissues. J. Pharmacol. Exp. Ther. 181, 339–345.

Hancock, A.A., Bush, E.N., Stanisic, D., Kyncl, J.J., Lin, C.T., 1988. Data normalization before statistical analysis: keeping the horse before the cart. Trends Pharmacol. Sci. 9, 29–32.

Hulme, E.C., Birdsall, N.J.M., 1992. Strategy and tactics in receptor-binding studies. In: Hulme, E.C. (Ed.), Receptor–Ligand Interactions. IRL Press at Oxford University Press, New York, pp. 63–176.

Kenakin, T.P., 1997. Pharmacologic Analysis of Drug–Receptor Interaction, third edn. Lippincott-Raven Press, New York.

Lanzafame, A., Christopoulos, A., Mitchelson, F., 1996. Interactions of agonists with an allosteric antagonist at muscarinic acetylcholine $M_2$ receptors. Eur. J. Pharmacol. 316, 27–32.

Lazareno, S., Birdsall, N.J.M., 1995. Detection, quantitation, and verification of allosteric interactions of agents with labelled and unlabelled ligands at G protein-coupled receptors: interactions of strychnine and acetylcholine at muscarinic receptors. Mol. Pharmacol. 48, 362–378.

Lee, N.H., El-Fakahany, E.E., 1991. Allosteric antagonists of the muscarinic acetylcholine receptor. Biochem. Pharmacol. 42, 199–205.

Leff, P., Prentice, D.J., Giles, H., Martin, G.R., Wood, J., 1990. Estimation of agonist affinity and efficacy by direct, operational model fitting. J. Pharmacol. Methods 23, 225–237.

Mitchelson, F., 1975. Antimuscarinic action of an alkane-bis-ammonium compound alone and in combination with (+)-benzetimide. Eur. J. Pharmacol. 33, 237–246.

Motulsky, H.J., 1995. Intuitive Biostatistics. Oxford Univ. Press, Oxford.

Motulsky, H.J., Ransnas, L.A., 1987. Fitting curves to data using nonlinear regression: a practical and nonmathematical review. FASEB J. 1, 365–374.

Munson, P.J., 1983. LIGAND: a computerized analysis of ligand binding data. Methods Enzymol. 92, 543–577.

Munson, P.J., Rodbard, D., 1980. LIGAND. A versatile computerized approach for the characterization of ligand binding systems. Anal. Biochem. 107, 220–239.

Parker, R.B., Waud, D.R., 1971. Pharmacological estimation of drug–receptor dissociation constants. Statistical evaluation: I. agonists. J. Pharmacol. Exp. Ther. 177, 1–12.

Stockton, J.M., Birdsall, N.J.M., Burgen, A.S.V., Hulme, E.C., 1983. Modification of the binding properties of muscarinic receptors by gallamine. Mol. Pharmacol. 23, 551–557.

Tucek, S., Proška, J., 1995. Allosteric modulation of muscarinic acetylcholine receptors. Trends Pharmacol. Sci. 16, 205–212.

Tucek, S., Musilkova, J., Nedoma, J., Proška, J., Shelkovnikov, S.W., Vorlicek, J., 1990. Positive cooperativity in the binding of alcuronium and *N*-methylscopolamine to muscarinic acetylcholine receptors. Mol. Pharmacol. 38, 674–680.

Waelbroeck, M., Tastenoy, M., Camus, J., Christophe, J., 1990. Binding of selective antagonists to four muscarinic receptors ($M_1$ to $M_4$) in rat forebrain. Mol. Pharmacol. 38, 267–273.

Waud, D.R., 1975. Analysis of dose–response curves. In: Daniel, E.E., Paton, M. (Eds.), Methods in Pharmacology: Smooth Muscle, Vol. 3. Plenum, New York, pp. 471–506.

Waud, D.R., 1987. Model building and dose–response curves. In: Black, J.W., Jenkinson, D.H., Gerskowitch, V.P. (Eds.), Perspectives on Receptor Classification. Alan R. Liss, New York, pp. 139–156.

Waud, D.R., Parker, R.B., 1971. Pharmacological estimation of drug–receptor dissociation constants. Statistical evaluation: II. Competitive antagonists. J. Pharmacol. Exp. Ther. 177, 13–24.

Waud, D.R., Son, L.S., Waud, B.E., 1978. Kinetic and empirical analysis of dose–response curves illustrated with a cardiac example. Life Sci. 22, 1275–1286.